PD-Activity in Generator Stator Bar insulation versus Voltage Frequency and Temperature

T.G. Aakre and E Ildstad
NTNU – Department of Electric Power Engineering
Trondheim, Norway

***Abstract-* Condition assessment of generators is today performed at various voltage frequencies and test temperatures. The main purpose of this paper is to compare measured PD results from sections of generator bars with that of similar tests performed on laboratory made test objects with void enclosures of known geometry. All test objects were subjected to voltage frequency in the range from 0.1 to 50 Hz (to 300 Hz for the smaller laboratory made test objects) to a maximum voltage of 10 kV, and test temperature in the range of 20° to 155°C. The measured PD characteristics were compared to estimated values using an impedance abc-model, including both conduction and dielectric response. At temperatures above 130 °C the measured partial discharge inception value (PDIV) was found to decrease with increasing temperature, particularly so at the lowest test frequencies. A mechanism caused by increased conductivity and higher rate of polarization at increased temperatures. The magnitude of the measured apparent charge was varying, strongly indicating that several discharges are needed for a complete discharge of a void.**

I. INTRODUCTION

Condition assessment of generators are today performed at different voltage frequencies. This means that condition assessment standards for hydropower generator stator insulation [1, 2] developed for power frequency testing are used for both low frequency (VLF) and 400 Hz testing. Online tests are performed during service at 50/60 Hz, whereas it during offline testing can be preferable to apply 0.1 Hz test voltage due to the large capacitance (0.5 to 3 μF) of the test object. In practice the generator temperature varies with cooling and current load variations making it difficult to perform condition assessment at the same stator temperature.

Detection of partial discharges (PDs) characteristics is a popular diagnostic method used to reveal the development of voids within the insulation. It is therefore important to know how typical insulation defects affect the measurable partial discharge parameters as for example; inception voltage, number and distribution of apparent charge magnitude.

The main purpose of this paper is to present and compare results from PD characterization performed on laboratory made test object with defined voids and sections of service aged generator bars.

II. THEORETICAL MODELS

The three electrical equivalent circuits used to model the test objects are shown in Fig. 1. Model 1 represents the classical capacitive abc-model, Model 2 includes resistances in parallel with the void and the insulation sections while Model 3 is based upon considering each component with its impedance including frequency dependent dielectric response.

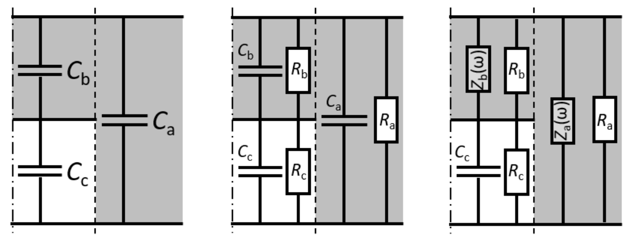

Fig. 1. Three electrical models used for pd-modelling of test object, a) represents the classical capacitive abc-model b) resistance and c) the impedance model.

A. *Partial Discharge Inception Voltage (PDIV)*

How the voltage across the void U_v varies with the applied voltage $U_\mathrm{a}$and frequency is determined by the electrical model used to describe the test object. The relation between the applied voltage U_a and the void voltage U_c is then given by the following equations [3]:

Model 1:

$$U_\mathrm{void} = \frac{1}{1+\dfrac{d_\mathrm{b}}{d_\mathrm{c}}\dfrac{\varepsilon_\mathrm{r,c}}{\varepsilon_\mathrm{r,b}}}\cdot U_\mathrm{applied} \tag{1}$$

$$U_\mathrm{a} = (1+\frac{d_\mathrm{b}}{d_\mathrm{c}}\frac{\varepsilon_\mathrm{r,c}}{\varepsilon_\mathrm{r,b}})\cdot U_\mathrm{c}$$

Model 2:

$$U_\mathrm{void} = \frac{1}{1+\dfrac{d_\mathrm{b}}{d_\mathrm{c}}\dfrac{\sigma_\mathrm{c}+j\omega\varepsilon_0\varepsilon_\mathrm{r,c}}{\sigma_\mathrm{b}+j\omega\varepsilon_0\varepsilon_\mathrm{r,b}}}\cdot U_\mathrm{applied} \tag{2}$$

$$U_\mathrm{a} = (1+\frac{d_\mathrm{b}}{d_\mathrm{c}}\frac{\sigma_\mathrm{c}+j\omega\varepsilon_0\varepsilon_\mathrm{r,c}}{\sigma_\mathrm{b}+j\omega\varepsilon_0\varepsilon_\mathrm{r,b}})\cdot U_\mathrm{c}$$

Model 3:

$$U_\mathrm{void} = \frac{1}{1+\dfrac{d_\mathrm{b}}{d_\mathrm{c}}\dfrac{\sigma_\mathrm{c}+j\omega\varepsilon_0\varepsilon_\mathrm{r,c}}{\sigma_\mathrm{b}-\omega\mathrm{Im}\{\varepsilon_\mathrm{b}^*\}+j\omega\mathrm{Re}\{\varepsilon_\mathrm{b}^*\}}}\cdot U_\mathrm{a} \tag{3}$$

$$U_{\mathrm{a}} = (1 + \frac{d_{\mathrm{b}}}{d_{\mathrm{c}}} \frac{\sigma_{\mathrm{c}} + j\omega\varepsilon_0\varepsilon_{\mathrm{r,c}}}{\sigma_{\mathrm{b}} - \omega \mathrm{Im}\{\varepsilon_{\mathrm{b}}^*\} + j\omega \mathrm{Re}\{\varepsilon_{\mathrm{b}}^*\}}) \cdot U_{\mathrm{c}} \tag{4}$$

where the subscripts b and c represent the series insulation and void respectively, d is the thickness, ε_r is the relative permittivity, σ is the conductivity, ω is the angular frequency, and ε^* is the complex permittivity.

Thus, the expected values of partial discharge inception voltages can be estimated using the above expressions and the assumption that a partial discharge occurring when the void voltage exceeds the breakdown voltage estimated by the Paschen curve [4]:

$$U_{\mathrm{s}} = 6.72\sqrt{pd} + 24.36(pd)[\mathrm{kV}], \tag{5}$$

with pressure times distance, pd, in the range 10^{-2} to $5 \cdot 10^{2}$ (bar cm). It is here assumed that the void voltage U_{void} equals the Paschen voltage at the PD inception voltage.

B. Apparent Charge

The duration of an internal void discharge is extremely short compared to the time variations of the applied voltage. Thus, the voltage distributions immediately after a discharge are well described by a pure capacitive abc model. The voltage drop occurring across the void results in a measurable external representing the apparent charge q_{a} needed to restore the voltage across the test object:

$$q_{\mathrm{a}} = C_{\mathrm{b}} \cdot (U_{\mathrm{s}} - U_{\mathrm{r}}), \tag{6}$$

Here C_{b} is the series capacitance to the void area with breakdown, U_{s} is the void breakdown voltage, and U_{r} is the remnant void voltage after the PD.

At an applied voltage of U_{applied}, the corresponding void voltage U_{void} is given by Equations (1), (2), and (3), depending on the magnitude of the material properties. The expected repetition number of PDs per voltage period is

$$n = 4 \cdot \frac{U_{\mathrm{void}} - U_{\mathrm{r}}}{U_{\mathrm{s}} - U_{\mathrm{r}}}. \tag{7}$$

III. Objects and Test Procedures

The dimensions of the laboratory made test objects and the generator bar samples are sketched in Fig. 2. The laboratory type test object was made of two 1.5 mm thick parallel plates, using a commercial epoxy/mica tape Samicatherm. One of the plates was made with a 0.5 mm deep indent forming the void when assembling the cured plates. The two plates were pressed together during PD testing. A reference sample without void was used to clearly distinguish void discharges from any external electrode and surface discharges.

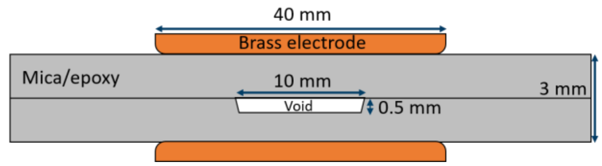

a) Laboratory made [Not to scale] 3 mm thick object with a void with diameter of 10 mm and a gap distance of 0.5 mm.

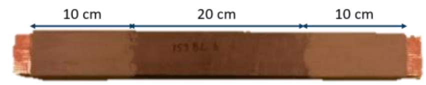

b) Examined section of service aged generator bars

The examined generator bars had been in service for 35 years and were as indicated in Fig. 2b sectioned into 40 cm long samples. The cross section of the bar is 20 mm x 56 mm. The main purpose of this was to facilitate high frequency testing and enable to put the samples into a small temperature controlled oven. Three test object of each type were examined.

The insulation materials were characterized with respect to its frequency dependent permittivity (dielectric response) in the frequency range from 10^{-4} and 10^{3} Hz using IDAX at 200 V_{peak}. The measure region was guarded. For the laboratory object, a grounded guard ring around the circular measure electrode was applied, whereas the field grading region of the generator bars were similarly connected directly to ground when measuring on the straight section of the bar. The test temperatures in this study were in the range of 20° to the insulation class design temperature 155°C.

The experimental PD setup is based on the direct measuring principle, as sketched in Fig. 3. This is based on a standard test circuit, also found in for example IEC 60034-27. The test setup is the same as is presented in our previous publication [3].

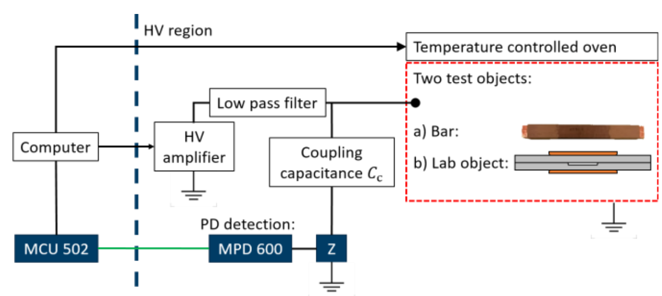

Fig. 3. Test setup for PD measurements

The voltage source, heat control, and data measurements were fully automated using LabView. The test procedure was based on the standard method in IEC 60034-27 and IEEE 1434 [1,2]. The standardised procedure at 50 Hz was expanded to a frequency and temperature sweep, with the intention to keep the PD characteristics at 50 Hz the same during the test. The test procedure used including several voltage frequencies is summarized in Fig. 4. Prior to testing a preconditioning period of 5 minutes at the maximum test voltage of 10 kV_{rms} at 50 Hz was applied to all test objects. During PD-testing the ac voltage was increased in ten equal steps to the maximum test voltage and then reduced to zero using the same ten voltage steps. The duration of each voltage step was the longer time of 10 s and 10 voltage periods. At low frequencies 10 periods were chosen as a minimum. In order to test if the test procedure itself had caused any change in PD void activity a reference test at 50 Hz PDIV was examined after each voltage /frequency sweep. The duration of this 50 Hz period was reduced to 5 s. When changing the temperature a stabilising time of 2 h was chosen before proceeding the electrical tests.

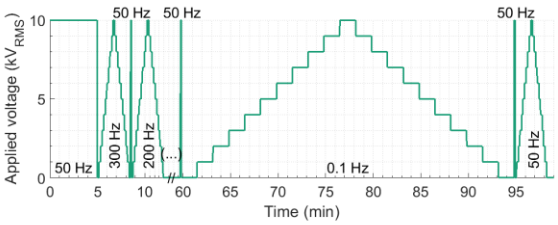

Fig. 4. Sketch of the voltage application frequency sweep with reducing frequency. This sketched procedure was used on the laboratory objects, whereas the start frequency for the bars was 50 Hz due to a higher capacitance and limited available current in the voltage source.

IV. Results

The PD inception voltage (PDIV) is here defined as the first (lowest) voltage that produces PDs with a magnitude larger than 100 pC. This value was chosen to be above the system sensitivity of 50 pC. The experimental results from both laboratory objects and generator bars are presented in Fig. 5. This figure also includes the estimated PDIV values based upon Model 3, including the measured dielectric response of the materials. The void conductivity was not measured, but estimated based on a curve fit to Model 3. The void conductivity in the model was insignificant and fixed at 0 S/m, expect at 20° and 40°C for the laboratory objects, where a high conductivity of 2 to 45 nS/m was needed to fit the results.

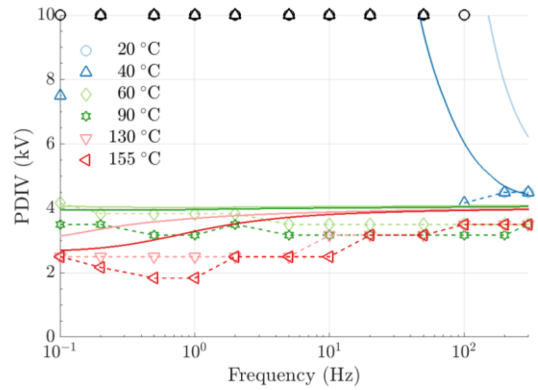

a) Laboratory object with void diameter of 10 mm and void gap distance of 0.5 mm. Black markers at 10 kV indicates no PDIV measured.

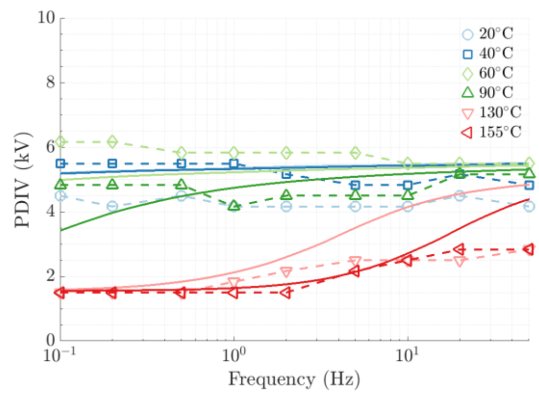

b) Bars close to the high voltage terminal. The void gap distance d_c was adjusted to 0.3 mm to correlate model and experimental results.

Fig. 5. PDIV at indicated temperatures as a function of voltage frequency. The solid lines represent Model 3 based on measured complex permittivity, and estimated void conductivity in the case of 20° and 40°C for laboratory objects.

The measured apparent charge distribution for the laboratory test objects and the generator bar sections are are presented in Fig. 6 as PD repetition rate per period versus PD magnitude. In the case of the laboratory test object, with predefined void area and gap distance, the PD repetition rate is expected to be 10 indicated in fig 6a. It is not possible to estimate an expected PD repetition rate for the generator bars due to the unknown number and size of voids. The results, however, clearly show a distribution of PD repetition rate for both type of test objects.

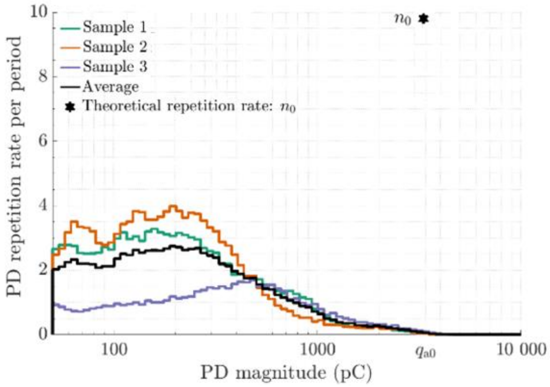

a) Laboratory object with void diameter of 10 mm and void gap distance of 0.5 mm. The expected PD repetition rate is indicated by a star.

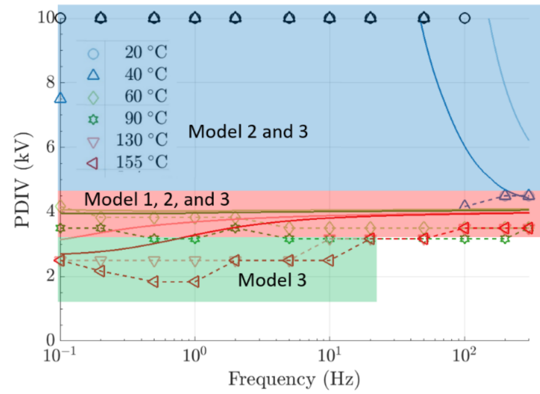

a) Laboratory object with void diameter of 10 mm and void gap distance of 0.5 mm. Black markers at 10 kV indicates no PDIV measured.

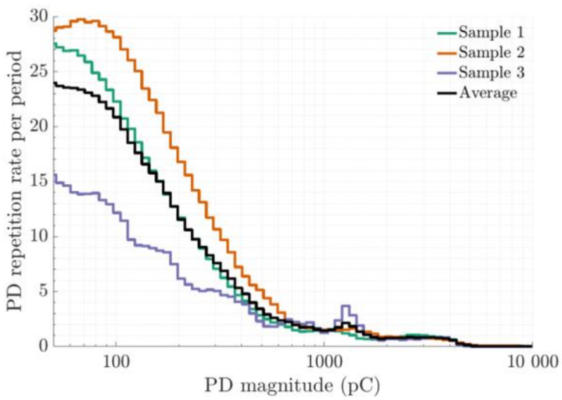

b) Bars close to the high voltage terminal. The void gap distance d_c was adjusted to 0.3 mm to correlate model and experimental results.

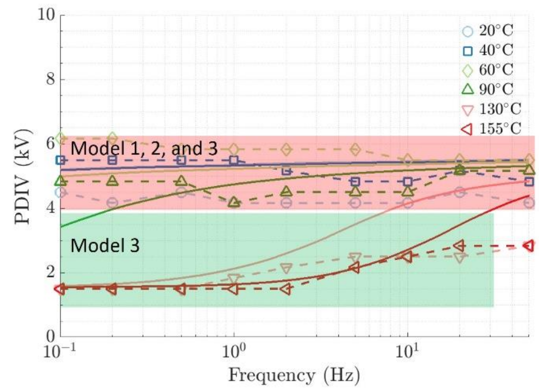

b) Bars close to the high voltage terminal. The void gap distance d_c was adjusted to 0.3 mm to correlate model and experimental results.

Fig. 6. Measured PD repetition rate per period as a function of PD magnitude at 10 kV and 50 Hz.

Fig. 7. PDIV at indicated temperatures as a function of voltage frequency. The shaded areas represents where the different models are valid.

V. Discussion

The comparisons between observed and estimated PDIV values based upon the 3 suggested models are summarized in Fig. 7. It is shown that the Model 3 including conductivity and dielectric response agree particularly well with the reduced PDIV values measured at high temperatures and low frequencies. No PDIV was measured below 10 kV in the case of 20° and 40°C for the laboratory made objects. This can be explained by a high void conductivity in Model 2 and Model 3. Probably indicating initial effects caused by the preconditioning and test procedure itself. This was in [3] deduced to be correlated to the effect of preconditioning and PD by-products acting as charge carriers, hence increasing the void conductivity. The maximum test voltage was, however, too low to get a good comparison between measured values and estimated values from the model. In summary, the capacitive Model 1 sufficiently accurately describes the experimental results at temperatures below 100°C at all test frequencies.

The measured apparent charge repetition rates presented in Fig. 6a shows that even within a single void a distribution of PD magnitudes occur. Thus it appears to be no fundamental difference between the laboratory and the generator bar samples of which results are presented in Fig. 6a and Fig. 6b, respectively. The main difference is the larger number of small PDs in the generator compared to that of the lab sample with one large void only. This means that the capacitance in series with the void discharge (C_b of Equation (4)) is not determined by the geometrical capacitance of the entire void , but rather represents the capacitance area involved in the discharge. The observed distribution of PD repetition rate and magnitude indicate many small discharges in each void. This is reasonable as the assumption of conductive and equipotential void surfaces is likely not fulfilled due to uneven charge deposits and inhomogeneous E-field distributions. Thus, it is difficult to distinguish one large void from many smaller voids by results from PD measurements of magnitude and repetition rate.

V. CONCLUSIONS

- The conventional capacitive abc-model (Model 1) sufficiently accurately describes the observed PDIV values results at temperatures below 100°C at all test frequencies below 50 Hz.
- The PDIV values estimated using models including conductivity and dielectric response agree particularly well with the reduced PDIV values measured at high temperatures and low frequencies.
- The results strongly indicate that it is not possible to distinguish between one large void and many small voids based on PD measurements of apparent charge magnitude and repetition rate.

ACKNOWLEDGMENT

This work is funded by the project “Hydro generator Stator Winding Insulation Assessment”. The project is supported by The Research Council of Norway (Project No. 255099/E20), and industrial partners.

REFERENCES

[1] *IEC TS 60034-27:2006, Off-line partial discharge measurements on the stator winding insulation of rotating electrical machines*, 2006.

[2] *IEEE Std 1434-2014 (Revision of IEEE Std 1434-2000), IEEE Guide for the Measurement of Partial Discharges in AC Electric Machinery*, 2014.

[3] T. G. Aakre, E. Ildstad, and S. Hvidsten, "Partial Discharge Inception Voltage of Voids Enclosed in Epoxy/Mica versus Voltage Frequency and Temperature," *IEEE Transactions on Dielectrics and Electrical Insulation,* vol. 27, no. 1, pp. 190-197, 2020.

[4] E. Kuffel and W. S. Zaengl, *High-voltage engineering: fundamentals*. Pergamon Press, 1984.